Solvatochromism, halochromism, and preferential solvation of new dipolar guaiazulenyl 1,4-benzoquinone methides†

Gerhard Laus,*[a] Herwig Schottenberger,*[b] Klaus Wurst,[b] Johannes Schütz,[c]
Karl-Hans Ongania,[d] Ulrike Erika Ida Horvath[b] and Alexander Schwärzler[b]

[a] *Immodal Pharmaka GmbH, Bundesstrasse 44, 6111 Volders, Austria*
[b] *Institute of General, Inorganic, Theoretical Chemistry, University of Innsbruck, Innrain 52a, 6020 Innsbruck, Austria*
[c] *Institute of Pharmacy, University of Innsbruck, Innrain 52a, 6020 Innsbruck, Austria*
[d] *Institute of Organic Chemistry, University of Innsbruck, Innrain 52a, 6020 Innsbruck, Austria*

The synthesis and the solvatochromic properties of five dyes, obtained by condensation of guaiazulene with 4-hydroxybenzaldehydes, are described. Crystal structures of a quinoid dye and a phenolic dye precursor are presented. The dyes are sensitive to the dipolarity–polarizability of the medium and to the hydrogen-bond donor ability of protic solvents. Their solvatochromism is discussed in terms of Kamlet–Taft's π^* and α scales, and their difference in behaviour is interpreted. Alkali and alkaline earth metal salts effect halochromism, with one exception due to extreme steric hindrance. Thus, this dye is capable of measuring solvent polarities without sensing the presence of electrolytes. Preferential solvation of the dyes in a series of binary solvent mixtures is explained quantitatively by solvent-exchange models.

Introduction

Solvents influence reaction rates, equilibria, and mechanisms.[1] It is therefore of interest to understand solute–solvent interactions and measure them quantitatively. A widely used approach is UV-VIS absorption spectroscopy of solvatochromic dyes as solvent polarity indicators.[2] The shifts of the observed absorption maxima are results of solute–solvent interactions. Since different probes register different kinds of interactions, it is possible to separate contributions from dipolarity–polarizability, hydrogen-bond donor (HBD), and hydrogen-bond acceptor (HBA) capabilities of the solvent. It is also possible to study solvent–solvent interactions in binary mixtures, as well as solvent–metal and solute–metal interactions in electrolyte solutions. Therefore, new molecular probes are of interest, with controllable properties and tailor-made sensitivities toward these interactions. We do not intend to introduce another solvent polarity scale which has been discouraged.[3] The new guaiazulene dyes offer the advantage of solubility in a wide range of solvents as well as cheap and simple preparation by a two-step synthesis. A similar quinone methide has been formerly described only as an undesired by-product.[4]

Results and discussion

Synthesis

Condensation of guaiazulene with 4-hydroxybenzaldehydes in the presence of tetrafluoroboric acid readily gives the 3-[(4-hydroxyphenyl)methylene]guaiazulenium tetrafluoroborates **1**–**5** in high yields. These salts are quantitatively converted to the neutral 4-(guaiazulen-3-yl-methylene)cyclohexa-2,5-dien-1-ones **6**–**10** (Scheme 1).

Solvatochromism

Typically, *n*-electron donor–acceptor-substituted conjugated systems exhibit solvatochromism. The solvatochromism of

1-10	1/6	2/7	3/8	4/9	5/10
R	H	Me	OMe	*t*-Bu	Br

Scheme 1
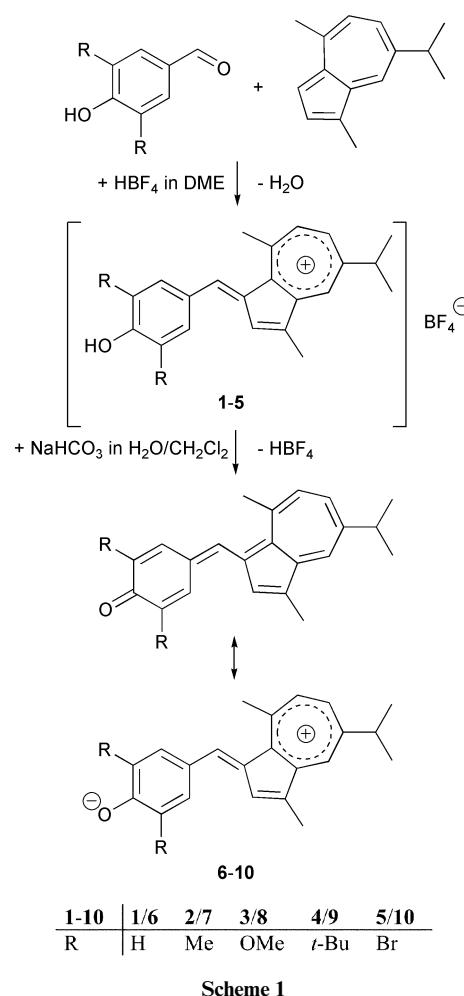
such systems arises from the different stabilization of their electronic ground and excited state by differential solvation of these two states, according to their different molecular and electronic structure. The electronic transition for **6**–**10** leads to more charge separation in the zwitterionic excited state than in the

less dipolar ground state, so that increased solvent polarity leads to lower transition energy (positive solvatochromism). Transition energies E_T are calculated from the wavelengths of the absorption maxima according to eqn. (1).

$$E_T/\text{kJ mol}^{-1} = hcN/\lambda = 119625/(\lambda/\text{nm}) \quad (1)$$

A linear solvation energy relationship is established by least-squares fitting the data to the solvatochromic eqn. (2),[5]

$$E_T = E_{T0} + s(\pi^* + d\delta) + aa + b\beta \quad (2)$$

involving the parameters π^*,[6] a,[7] and β[8] which represent the dipolarity–polarizability, HBD, and HBA capabilities of the solvent. The coefficients s, a, b, and d reflect the sensitivity of the solute to these solvent properties. The polarizability correction term δ was introduced to explain certain data in aromatic and polychloro solvents,[9] but is unnecessary for all electronic spectra that are shifted to lower frequencies with increasing solvent dipolarity;[3,6] it has been criticized as unwarranted,[10] but nevertheless found to be useful.[11] We found no reason to apply this correction. It was also our intent to avoid overparametrization. Thus, the simplified eqn. (3) adequately describes the behaviour of the quinoid dyes **6**–**10** as a function of π^* and a only.

$$E_T = E_{T0} + s\pi^* + aa \quad (3)$$

From the spectral data (Table 1) equations (4–8) were derived (standard errors of E_{T0}, s, and a, squared correlation coefficient r^2 of calculated *vs.* found values, residual standard deviation σ of the correlation, and number N of data points given). There were no statistically significant outliers.

For **6**:

$E_T/\text{kJ mol}^{-1} =$
$\qquad 244.4(\pm 0.9) - 21.0(\pm 1.3)\pi^* - 21.9(\pm 1.2)a \quad (4)$

$r^2 = 0.945$, $\sigma/\text{kJ mol}^{-1} = 2.19$ (rel. $\sigma = 0.96\%$), $N = 37$
For **7**:

$E_T/\text{kJ mol}^{-1} =$
$\qquad 245.8(\pm 0.6) - 18.2(\pm 0.9)\pi^* - 15.4(\pm 0.9)a \quad (5)$

$r^2 = 0.953$, $\sigma/\text{kJ mol}^{-1} = 1.62$ (rel. $\sigma = 0.70\%$), $N = 38$
For **8**:

$E_T/\text{kJ mol}^{-1} =$
$\qquad 246.8(\pm 0.9) - 19.1(\pm 1.4)\pi^* - 18.7(\pm 1.3)a \quad (6)$

$r^2 = 0.918$, $\sigma/\text{kJ mol}^{-1} = 2.47$ (rel. $\sigma = 1.06\%$), $N = 38$
For **9**:

$E_T/\text{kJ mol}^{-1} =$
$\qquad 246.3(\pm 0.4) - 14.9(\pm 0.6)\pi^* - 5.2(\pm 0.6)a \quad (7)$

$r^2 = 0.945$, $\sigma/\text{kJ mol}^{-1} = 1.15$ (rel. $\sigma = 0.49\%$), $N = 38$
For **10**:

$E_T/\text{kJ mol}^{-1} =$
$\qquad 222.4(\pm 0.4) - 20.1(\pm 0.7)\pi^* - 12.6(\pm 1.1)a \quad (8)$

$r^2 = 0.972$, $\sigma/\text{kJ mol}^{-1} = 1.12$ (rel. $\sigma = 0.53\%$), $N = 31$

The highest wavelength shifts were observed in the cases of the unsubstituted and the dimethoxy-substituted quinone methides **6** and **8**. Compound **9** showed rather weak solvatochromic effects, obviously for steric reasons of the *t*-butyl

substituents which hinder the solvation. Especially the HBD sensitivity is very low in **9** compared to the other indicator molecules.

The absorption band of the dibromo-substituted quinone methide **10** became very broad in polar solvents, accompanied by the appearance of a shoulder at a higher wavelength which in primary alcohols became a new maximum. These data were therefore not included in the correlation (*cf.* Table 1).

The phenolic cations **1**–**5** also showed solvatochromism which, however, could not be correlated satisfactorily with any solvent properties. Solubility of these salts in less polar solvents is very limited. In some solvents the cation **5** showed the spectrum of the corresponding quinone methide. It is also noteworthy that the direction of the solvatochromic shift is reversed, and the protonated solutes **1,2,3**, and **5** display negative solvatochromism. Surprisingly, the *t*-butyl cation **4** retains its positively solvatochromic behavior (Table 2).

Halochromism

The addition of electrolytes to solutions of halochromic solutes causes shifts of the absorption band similar to those observed on addition of polar solvents. Effects of iodides and perchlorates of alkali and alkaline earth metals on Reichardt's dye in acetonitrile,[12] alcohols,[13] and dipolar solvents[14] have been reported. Halochromism of other quinoid probes[15] as well as pure π^* probes[16,17] have also been investigated. A study showed the formation of different complexes between lithium ions and several indicator molecules in diethyl ether and tetrahydrofuran solutions depending on lithium concentrations.[18]

The guaiazulenylbenzoquinone methides exhibit positive halochromism, *i.e.* bathochromic band shifts are found with increasing salt concentrations c. The curves obtained show an initial decrease of the transition energy $E_{T,\,obs}$ and reach a plateau at higher electrolyte concentrations. The data can be described by the empirical eqn. (9)[13] which has originally been developed for binary solvent mixtures.[19]

$$E_{T,\,obs} = E_{T0} + A\,\ln\left(\frac{c}{c^*} + 1\right) \quad (9)$$

E_{T0} is the transition energy in the pure solvent, and the slope A of a linear plot of $E_{T,\,obs}$ *vs.* $\ln(c/c^* + 1)$ is obtained after adjustment of c^*. The parameter c^* has been defined as a threshold value between dilute and concentrated systems.[20] For very dilute salt solutions eqn. (10) is obtained.

$$\frac{dE_{T,\,obs}}{dc} = \frac{A}{c^*} \quad (10)$$

Table 3 lists the systems studied. The A, c^*, and A/c^* values are given, together with the concentration c range, and the statistical parameters r^2, σ, and N. The extent of the cationic halochromism was found to be in the order Li > Na > K > n-Bu$_4$N, whereas the effect of the anion was ClO$_4$ > I > Br > Cl. No anion effect was found with tetra-*n*-butylammonium iodide and bromide. The sensitivity of the compounds was **8** > **6** > **7**, whereas **9** was insensitive, and **10** produced band shapes similar to those in primary alcohols which did not permit evaluation. Interestingly, the dyes **6** and **8** were more sensitive to LiI in acetone, whereas compound **7** was more affected by LiI in acetonitrile. Ba, Sr, and Ca iodides effected extreme shifts of **6**–**8** in acetone, but also changed the band shapes similar to that of **10**. It is noteworthy that the *t*-butyl derivative **9** was completely unchanged even in saturated CaI$_2$ solution. Therefore, this dye gives the unique possibility of measuring solvent polarities without sensing the presence of electrolytes.

Preferential solvation

Many mixtures of organic solvents and water as well as organic–organic mixtures have been examined using 4-(2,4,6-

Table 1 Electronic absorption maxima and transition energies of the dyes **6**–**10** measured in thirty-eight solvents of different polarity

Solvent	$\pi^{*\,a}$	a^{a}	6 λ_{max}/nm	6 E_T/kJ mol^{-1}	7 λ_{max}/nm	7 E_T/kJ mol^{-1}	8 λ_{max}/nm	8 E_T/kJ mol^{-1}	9 λ_{max}/nm	9 E_T/kJ mol^{-1}	10 λ_{max}/nm	10 E_T/kJ mol^{-1}
Methanol	0.60	0.98	562.6	212.6	542.9	220.3	552.0	216.7	517.5	231.2	(630.0)	—[b]
Ethanol	0.54	0.86	556.4	215.0	535.4	223.4	541.2	221.0	511.8	233.7	(628.5)	—[b]
Propan-1-ol	0.52	0.84	555.8	215.2	535.4	223.4	542.4	220.5	510.8	234.2	(623.6)	—[b]
Propan-2-ol	0.48	0.76	552.4	216.6	531.6	225.0	531.6	225.0	506.5	236.2	586.5	204.0
Butan-1-ol	0.47	0.84	555.8	215.2	534.3	223.9	540.2	221.4	511.1	234.1	(622.0)	—[b]
t-Butanol	0.41	0.42	535.6	223.3	522.2	229.1	520.8	229.7	500.0	239.2	575.5	207.9
Butan-2-ol	0.40	0.69	550.0	217.5	530.2	225.6	530.0	225.7	506.5	236.2	583.0	205.2
Dichloromethane	0.82	0.13	533.8[c]	224.1	520.8[d]	229.7	525.8[e]	227.5	508.0[f]	235.5	583.5[g]	205.0
Acetonitrile	0.75	0.19	524.5	228.1	516.2	231.7	516.9	231.4	507.6	235.7	579.7	206.4
Acetone	0.71	0.08	517.6	231.1	511.2	234.0	507.8	235.6	503.5	237.6	573.0	208.8
Butan-2-one	0.67	0.06	517.8	231.0	511.8	233.7	506.4	236.2	504.5	237.1	572.8	208.8
Chloroform	0.58	0.20	533.7	224.1	521.4	229.4	528.2	226.5	508.0	235.5	580.8	206.0
N-Methylformamide	0.90	0.62	555.2	215.5	535.6	223.3	546.4	218.9	519.4	230.3	(634.4)	—[b]
Diiodomethane	1.12[h]	0	550.6	217.3	535.0	223.6	541.4	221.0	522.0	229.2	598.4	199.9
Nitrobenzene	1.01	0	540.6	221.3	530.0	225.7	532.6	224.6	522.8	228.8	(605.4)	—[b]
Dimethyl sulfoxide	1.00	0	536.4	223.0	529.6	225.9	527.6	226.7	517.0	231.4	(624.5)	—[b]
N,N-Dimethylformamide	0.88	0	528.2	226.5	523.0	228.7	520.6	229.8	513.8	232.8	587.0	203.8
N,N-Dimethylacetamide	0.88	0	527.6	226.7	519.0	230.5	515.6	232.0	512.0	233.6	581.4	205.8
Pyridine	0.87	0	531.6	225.0	522.8	228.8	522.6	228.9	516.0	231.8	587.5	203.6
Iodobenzene	0.81	0	531.8	224.9	520.8	229.7	521.8	229.3	514.8	232.4	584.4	204.7
Propionitrile	0.71	0	523.8	228.4	514.8	232.4	513.0	233.2	507.5	235.7	577.0	207.3
Chlorobenzene	0.71	0	523.8	228.4	513.4	233.0	516.4	231.7	509.8	234.7	578.8	206.7
Tri-n-butyl phosphate	0.65	0	512.6	233.4	509.2	235.1	502.2	237.9	503.4	237.8	568.4	210.1
Carbon disulfide	0.61	0	522.4	229.0	514.8	232.4	517.2	231.3	508.9	235.1	571.5	209.3
Benzene	0.59	0	512.6	233.4	503.8	237.4	502.8	237.9	501.5	238.5	563.8	212.2
Tetrahydrofuran	0.58	0	511.2	234.0	505.2	236.8	501.0	238.8	503.5	237.6	568.5	210.4
Ethyl acetate	0.55	0	508.0	235.5	502.8	237.9	499.2	239.6	499.3	239.6	563.8	212.2
Toluene	0.54	0	509.4	234.8	503.0	237.8	501.4	238.6	500.5	239.0	561.0	213.2
Trichloroethene	0.53	0	520.8	229.7	509.8	234.7	513.4	233.0	501.9	238.3	568.2	210.5
1,2-Dimethoxyethane	0.53	0	509.2	234.9	504.8	237.0	499.0	239.7	501.5	238.5	566.0	211.4
n-Butyl acetate	0.46	0	506.4	236.2	501.8	238.4	497.4	240.5	499.0	239.7	561.4	213.1
Tetrachloromethane	0.28	0	505.0	236.9	499.4	239.5	500.4	239.1	495.0	241.7	549.8	217.6
Diethyl ether	0.27	0	498.0	240.2	494.4	242.0	490.4	243.9	492.5	242.9	549.0	217.9
Triethylamine	0.14	0	493.6	242.4	490.9	243.7	489.7	244.3	488.5	244.9	543.0	220.3
Cyclohexane	0.00	0	490.6	243.8	489.0	244.6	488.2	245.0	489.2	244.5	541.4	221.0
n-Hexane	−0.04	0	485.2	246.5	483.4	247.5	484.0	247.2	485.0	246.6	535.5	223.4
n-Heptane	−0.08	0	488.6	244.8	486.2	246.0	486.4	245.9	485.0	246.6	536.6	222.9
Tetramethylsilane	−0.09	0	—[i]	—[i]	482.7	247.8	482.8	247.8	482.4	248.0	531.8	224.9

[a] Values taken from ref. 37. [b] Not used for correlation due to band shape problems. [c] Log ε/dm^3 mol^{-1} cm^{-1} 4.63. [d] Log ε/dm^3 mol^{-1} cm^{-1} 4.54. [e] Log ε/dm^3 mol^{-1} cm^{-1} 4.62. [f] Log ε/dm^3 mol^{-1} cm^{-1} 4.62. [g] Log ε/dm^3 mol^{-1} cm^{-1} 4.60. [h] From ref. 5. [i] Insoluble.

Table 2 Electronic absorption maxima and transition energies of the cationic dyes **1**–**5** in eighteen solvents of different polarity

Solvent	π^{*a}	α^a	β^a	**1** λ_{max}/nm	E_T/kJ mol^{-1}	**2** λ_{max}/nm	E_T/kJ mol^{-1}	**3** λ_{max}/nm	E_T/kJ mol^{-1}	**4** λ_{max}/nm	E_T/kJ mol^{-1}	**5** λ_{max}/nm	E_T/kJ mol^{-1}
Formic acid	0.65	1.23	0.38	509.0	235.0	526.6	227.2	532.8	224.5	531.6	225.0	481.4	248.5
Acetic acid	0.64	1.12	0.45	520.2	230.0	534.2	223.9	557.0	214.8	528.6	226.3	484.2	247.1
Methanol	0.60	0.98	0.66	526.4	227.3	544.2	219.8	567.8	210.7	516.0	231.8	496.5	240.9
Ethanol	0.54	0.86	0.75	535.0	223.6	551.0	217.1	575.2	208.0	514.2	232.6	508.6	235.2
Propan-1-ol	0.52	0.84	0.90	540.4	221.4	557.0	214.8	583.2	205.1	513.8	232.8	511.6	233.8
Propan-2-ol	0.48	0.76	0.84	540.8	221.2	553.2	216.2	555.0	215.5	506.2	236.3	526.5	227.2
Butan-1-ol	0.47	0.84	0.84	545.8	219.2	559.2	213.9	590.4	202.6	510.8	234.2	521.8	229.3
Butan-2-ol	0.40	0.69	0.80	546.6	218.9	540.8	221.2	550.6	217.3	506.2	236.3	533.0	224.4
Acetonitrile	0.75	0.19	0.40	511.4	233.9	525.6	227.6	543.0	220.3	524.5	228.1	481.8	248.3
Acetone	0.71	0.08	0.43	518.8	230.6	531.6	225.0	555.8	215.2	526.6	227.2	488.0	245.1
Dichloromethane	0.82	0.13	0.10	526.0^c	227.4	534.0^d	224.0	564.0^e	212.1	548.2^f	218.2	493.0^g	242.6
Chloroform	0.58	0.20	0.10	553.6	216.1	527.6	226.7	563.8	212.2	532.8	224.5	485.6	246.3
Dimethyl sulfoxide	1.00	0	0.76	535.0	223.6	525.6	227.6	527.8	226.6	517.5	231.2	(622.5)	—^{b}
Propionitrile	0.71	0	0.39	519.8	230.1	510.0	234.6	513.2	233.1	505.0	236.9	(577.5)	—^{h}
Tetrahydrofuran	0.58	0	0.55	524.4	228.1	503.8	237.4	502.0	238.3	502.2	238.2	(568.4)	—^{h}
1,2-Dimethoxyethane	0.53	0	0.41	—^{i}	—^{i}	—^{i}	—^{i}	—^{i}	—^{i}	500.2	239.2	—^{i}	—^{i}
Ethyl acetate	0.55	0	0.45	505.4	236.7	503.0	237.8	499.0	239.7	499.0	239.7	(561.2)	—^{h}
Diethyl ether	0.27	0	0.47	—^{i}	—^{i}	—^{i}	—^{i}	—^{i}	—^{i}	492.0	243.1	—^{i}	—^{i}

^{a} Values taken from ref. 37. ^{b} Not used for correlation due to band shape problems. ^{c} Log ε/dm^3 mol^{-1} cm^{-1} 4.73. ^{d} Log ε/dm^3 mol^{-1} cm^{-1} 4.56. ^{e} Log ε/dm^3 mol^{-1} cm^{-1} 4.54. ^{f} Log ε/dm^3 mol^{-1} cm^{-1} 4.75. ^{g} Log ε/dm^3 mol^{-1} cm^{-1} 4.51. ^{h} Value of the corresponding quinone methide. ^{i} Insoluble.

Table 3 Halochromic parameters of the dyes **6**–**8**^{a} for eleven electrolyte solutions

Salt–solvent	**6** A/kJ mol^{-1}	c^*/mol dm^{-3}	(A/c^*)/kJ dm^3 mol^{-2}	**7** A/kJ mol^{-1}	c^*/mol dm^{-3}	(A/c^*)/kJ dm^3 mol^{-2}	**8** A/kJ mol^{-1}	c^*/mol dm^{-3}	(A/c^*)/kJ dm^3 mol^{-2}
LiClO$_4$–acetone	−30.52 c = 0–0.1 M, r^2 = 0.992, N = 6	0.54	−57	−7.15 c = 0–0.12 M, r^2 = 0.994, N = 7	0.097	−74	−37.33 c = 0–0.12 M, r^2 = 0.994, N = 7	0.18	−207
LiI–acetone	−15.15 c = 0–0.12 M, r^2 = 0.983, N = 7	0.064	−237	−3.68 c = 0–0.12 M, r^2 = 0.982, N = 7	0.031	−119	−33.09 c = 0–0.12 M, r^2 = 0.998, N = 7	0.15	−221
LiBr–acetone	−1.79 c = 0–0.1 M, r^2 = 0.993, N = 6	0.0092	−195	−1.50 c = 0–0.1 M, r^2 = 0.998, N = 6	0.025	−60	−3.02 c = 0–0.1 M, r^2 = 0.968, N = 6	0.025	−121
LiCl–acetone	−0.80 c = 0–0.1 M, r^2 = 0.999, N = 5	0.0056	−143	—^{b}			−0.87 c = 0–0.08 M, r^2 = 0.997, N = 5	0.0098	−89
NaI–acetone	—^{b}			—^{b}			−7.88 c = 0–0.12 M, r^2 = 0.996, N = 7	0.033	−239
KI–acetone	—^{b}			—^{b}			−1.40 c = 0–0.03 M, r^2 = 0.989, N = 6	0.0061	−230
n-Bu$_4$NI–acetone	—^{b}			—^{b}			—^{b}		
n-Bu$_4$NBr–acetone	—^{b}			—^{b}			—^{b}		
LiI–acetonitrile	−3.76 c = 0–0.12 M, r^2 = 0.977, N = 8	0.0010	−3760	−10.32 c = 0–0.12 M, r^2 = 0.958, N = 7	0.040	−258	−8.11 c = 0–0.09 M, r^2 = 0.981, N = 6	0.0045	−1802
NaI–acetonitrile	—^{b}			—^{b}			−6.63 c = 0–0.1 M, r^2 = 0.994, N = 11	0.022	−301
KI–acetonitrile	—^{b}			—^{b}			−1.24 c = 0–0.06 M, r^2 = 0.964, N = 8	0.0056	−221

^{a} The concentration of the dye was 1×10^{-5} mol dm^{-3}. ^{b} No significant halochromic shift observed.

triphenylpyridinium-1-yl)-2,6-diphenyl phenolate ('Reichardt's Dye'),[21,22] 2,6-dichloro-4-(2,4,6-triphenylpyridinium-1-yl)phenolate,[23] 4-nitroanisol, 4-nitroaniline, *N*,*N*-diethyl-4-nitroaniline,[24] 4-nitrophenol, β-carotene,[25] 1-ethyl-4-(methoxycarbonyl)pyridinium iodide,[26] 5-(dimethylamino)-5′-nitro-2,2′-bithiophene,[16] 2,3-diaryltetrazolium-5-thiolates,[27] *N*-ethyl-4-cyanopyridinium iodide,[28] dicyano(1,10-phenanthroline)-iron(II),[29] aryliminomethylpyridinium iodides[30], *N*-4-(dimethyl-aminophenyl)-1,4-benzoquinoneimine (Phenol Blue)[31] as solvatochromic indicators. The validity of solvatochromic indicator solutes for the characterization of mixed solvents has been discussed.[25] Several theoretical models have been compared.[32]

Preferential solvation denotes the deviation from ideal behaviour (eqn. 11), *i.e.* when the observed transition energies vary non-linearly with the bulk composition (mole fractions X_1 and X_2) of binary mixtures.

$$E_{T, obs} = X_1 E_{T1} + X_2 E_{T2} \qquad (11)$$

When a solute is dissolved in a solvent mixture, the microsphere of solvation contains the local mole fractions of the two components of the mixture, x_1 and x_2. Then, $E_{T, obs}$ is given by eqn. (12) and x_1, by eqn. (13).

$$E_{T, obs} = x_1 E_{T1} + x_2 E_{T2} \qquad (12)$$

$$x_1 = \frac{E_{T, obs} - E_{T2}}{E_{T1} - E_{T2}} \qquad (13)$$

An early solvent-exchange model[33] postulated the presence of several different solvational species in the solution. This model has been criticized[34] on grounds that, according to the Beer–Lambert law and Frank–Condon principle, for mixtures of two or more chromophores the absorption spectra of the individual components must be added, not averaged. Rather, the situation should be regarded as a solvent-exchange equilibrium between the bulk and the solvation microsphere, as shown in eqn. (14), resulting in only one solute species with a defined solvation shell.

$$S_2(bulk) + S_1(microsphere) \rightleftharpoons$$
$$S_1(bulk) + S_2(microsphere) \quad (14)$$
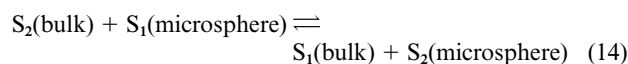
A plot of (x_2/x_1) *vs.* (X_2/X_1) gives a straight line with slope $f_{2/1}$ (eqn. 15), the preferential solvation constant (also termed K_{PS}). Then, $E_{T, obs}$ is given by eqn. (16).

$$f_{2/1} = \frac{x_2 X_1}{x_1 X_2} \qquad (15)$$

$$E_{T, obs} = E_{T1} + \frac{f_{2/1}(E_{T2} - E_{T1})X_2}{X_1 + f_{2/1}X_2} \qquad (16)$$

Obviously, this simple model gives good fits in cases when the polarity of the mixture is in between that of the two pure solvents (Table 4). When non-linearity of a plot of (x_2/x_1) *vs.* (X_2/X_1) is found,[35] $f_{2/1}$ cannot be determined in a simple manner.

In the event of strong solvent–solvent interactions the appearance of an extremum in an intermediate composition leads to the unsatisfactory situation of $x_2 > 1$ (and thus x_1 negative).[29] In this case, the formation of a H-bonded solvent structure, sometimes more polar than any of the two pure solvents mixed, is postulated. It is assumed that the two solvents

interact in the ratio of 1 : 1 to form the solvent–cosolvent complex according to eqn. (17).[21]

$$S_1 + S_2 \rightleftharpoons 2S_{12} \qquad (17)$$

The equilibrium constant of this process is given by eqn. (18).

$$K_{12} = \frac{X_{12}^2}{X_1 X_2} \qquad (18)$$

The relationship between the molar fraction of the species involved is given in eqn. (19), X_{01} and X_{02} being the molar fractions of the pure solvents mixed, X_1, X_2, and X_{12} the molar fractions of the solvent species in the bulk mixture, and x_1, x_2, and x_{12} the corresponding molar fractions in the solvation shell.

$$X_{01} + X_{02} = X_1 + X_2 + X_{12} = x_1 + x_2 + x_{12} \qquad (19)$$

The molar fraction of the solvent–cosolvent complex in the bulk is obtained from eqn. (20),

$$X_{12} = \frac{K_{12}}{K_{12} - 4} \pm \sqrt{\left(\frac{K_{12}}{K_{12} - 4}\right)^2 - 4\frac{K_{12}}{K_{12} - 4}X_{01}X_{02}} \qquad (20)$$

the sign of the square root depending on the size of K_{12} (negative if $K_{12} > 4$, positive if $K_{12} < 4$) to obtain meaningful values of X_{12}, *i.e.* $0 < X_{12} < 1$. Then the transition energy observed can be calculated as the weighted average of the transition energies in pure solvents according to their local molar fractions in the solvation sphere of the dye molecule, as given by eqn. (21)

$$E_{T, obs} = x_1 E_{T1} + x_2 E_{T2} + x_{12} E_{T12} \qquad (21)$$

The preferential solvation parameters $f_{2/1}$ and $f_{12/1}$ are defined in eqns. (15) and (22), respectively.

$$f_{12/1} = \frac{x_{12} X_1}{x_1 X_{12}} \qquad (22)$$

Substituting and rearranging leads to eqn. (23), which describes $E_{T, obs}$ as a function of X_{02}, with the constants $f_{2/1}, f_{12/1}, K_{12}$ (and thus X_{12}), and E_{T12} to be determined.

$$E_{T, obs} = E_{T1} +$$
$$\frac{f_{2/1}(E_{T2} - E_{T1})X_{02} + \left(f_{12/1}(E_{T12} - E_{T1}) - \frac{f_{2/1}(E_{T2} - E_{T1})}{2}\right)X_{12}}{1 + (f_{2/1} - 1)X_{02} + \left(f_{12/1} - \frac{1 + f_{2/1}}{2}\right)X_{12}}$$
$$(23)$$

However, the necessary refinement of four parameters can lead to ambiguous results. For example, the preferential solvation of the dimethoxy quinone methide **8** in chloroform–methanol can be described almost equally well by two very different sets of parameters, (a) $E_{T12} = 186$ kJ mol^{-1}, $f_{2/1} = 0.47$, $f_{12/1} = 0.45$, $K_{12} = 3.96$ with the coefficient of correlation $r^2 = 0.999$, or (b) $E_{T12} = 200$ kJ mol^{-1}, $f_{2/1} = 0.11$, $f_{12/1} = 0.73$, $K_{12} = 7.05$ with $r^2 = 0.998$. It cannot be readily determined which K_{12} value is correct. For this reason, this model was abandoned although the theory behind it is straightforward and logical.

Since $E_{T, obs}$ is sensitive to the proportions of solvents S_1, S_2, and S_{12} in the solvation microsphere, but not to their proportions in the bulk solvent, it may be assumed that the 'mixed' solvent S_{12} is formed in the microsphere of solvation of the indicator,[21] which is certainly another simplification. In this

Table 4 Preferential solvation parameters of the dyes **6**–**10** in seven binary solvent mixtures

Solvent 1–solvent 2	Compound	E_{T12}^a	$f_{2/1}^a$	$f_{12/1}^a$	$X_{iso}(1)$	σ (rel. σ)^d	r^2
Ethyl acetate–chloroform	**6**	227.0	1.39	1.83	0.63	0.22 (0.097%)	0.997
			1.78^b		0.64	0.29 (0.12%)	0.995
	7	231.4	1.37	2.34	0.66	0.16 (0.067%)	0.997
			1.98^b		0.66	0.16 (0.067%)	0.997
	8	228.4	1.43	3.49	0.75	0.22 (0.095%)	0.998
			2.92^b		0.74	0.22 (0.096%)	0.998
	9	237.4	1.00	1.41	0.51	0.18 (0.076%)	0.986
			1.06^b		0.51	0.19 (0.081%)	0.984
	10	208.3	1.39	2.36	0.60	0.15 (0.072%)	0.995
			1.51^b		0.60	0.15 (0.073%)	0.995
Tri-*n*-butyl phosphate–chloroform	**6**	229.0	0.81	0.91	—^{c}	0.18 (0.079%)	0.998
	7	233.4	0.98	0.40	—^{c}	0.16 (0.069%)	0.995
	8	230.9	0.99	0.89	—^{c}	0.16 (0.068%)	0.999
	9	239.4	0.91	0.82	0.26	0.071 (0.030%)	0.992
	10	211.7	1.01	0.79	0.35	0.063 (0.030%)	0.999
Acetone–chloroform	**6**	220.8	2.27	1.09	0.74	0.18 (0.080%)	0.996
	7	226.9	1.06	1.62	0.78	0.13 (0.059%)	0.995
	8	223.1	2.26	1.81	0.79	0.28 (0.12%)	0.994
	9	234.8	0.57	1.55	0.71	0.12 (0.051%)	0.981
	10	203.3	0.54	1.33	0.80	0.11 (0.053%)	0.992
Chloroform–methanol	**6**	210.8	2.35	12.8	0.94	0.20 (0.094%)	0.997
	7	215.7	0.62	4.54	0.90	0.29 (0.14%)	0.994
	8	214.2	0.41	3.03	0.82	0.092 (0.042%)	0.999
	9	227.3	1.21	3.15	0.90	0.096 (0.042%)	0.998
Acetone–methanol	**6**	217.4	2.26	2.22	0.68	0.31 (0.14%)	0.998
			2.25^b		0.69	0.50 (0.22%)	0.994
	7	224.0	1.70	2.01	0.65	0.23 (0.10%)	0.998
			1.93		0.66	0.30 (0.13%)	0.996
	8	226.2	1.56	2.90	0.55	0.13 (0.055%)	1.000
			1.23^b		0.55	0.21 (0.093%)	0.999
	9	236.1	1.33	3.76	0.35	0.25 (0.11%)	0.986
			0.55^b		0.36	0.27 (0.12%)	0.984
Acetonitrile–butan-1-ol	**6**	215.5	8.24	3.58	0.83	0.28 (0.13%)	0.996
	7	222.6	5.65	2.66	0.83	0.11 (0.048%)	0.999
	8	226.9	6.71	7.89	0.69	0.18 (0.080%)	0.997
	9	233.5	0.76	3.33	0.85	0.10 (0.043%)	0.971
Benzene–propan-2-ol	**6**	216.4	0.45	5.70	0.88	0.37 (0.17%)	0.995
	7	224.8	1.35	6.06	0.87	0.21 (0.092%)	0.998
			6.99^b		0.87	0.27 (0.11%)	0.996
	8	225.1	1.59	5.21	0.84	0.24 (0.10%)	0.997
			5.33^b		0.84	0.25 (0.11%)	0.997
	9	235.0	1.19	4.64	0.88	0.10 (0.043%)	0.991
	10	203.0	0.47	3.64	0.84	0.13 (0.063%)	1.000

^{a} From eqn. (26) unless stated otherwise. ^{b} From eqn. (16). ^{c} Dual behaviour. ^{d} $N = 11$.

model, the preferential solvation parameters $f_{2/1}$ and $f_{12/1}$ are defined in eqns. (24) and (25).

$$f_{2/1} = \frac{x_2 X_1^2}{x_1 X_2^2} \quad (24)$$

$$f_{12/1} = \frac{x_{12} X_1}{x_1 X_2} \quad (25)$$

The resulting eqn. (26) gives excellent fits to the solvatochromic data.

$$E_{T,\,obs} = E_{T1} + \frac{f_{2/1}(E_{T2} - E_{T1})X_2^2 + f_{12/1}(E_{T12} - E_{T1})X_1 X_2}{X_1^2 + f_{2/1}X_2^2 + f_{12/1}X_1 X_2} \quad (26)$$

In this model only three parameters have to be iterated to minimize the sum of squared residuals, and no ambiguities were encountered. The results are presented in Table 4. Wavelengths of the absorption maxima and $E_{T,\,obs}$ values are deposited as Electronic Supplementary Information (Table S1)†. The isosolvation (or equisolvation) point X_{iso} may be used to describe the shape of the curve regardless which model is used to explain the data. X_{iso} is the composition at which $E_{T,\,obs}$ lies midway between the values of the pure solvents. The curves obtained are shown in Figs. 1–7. The
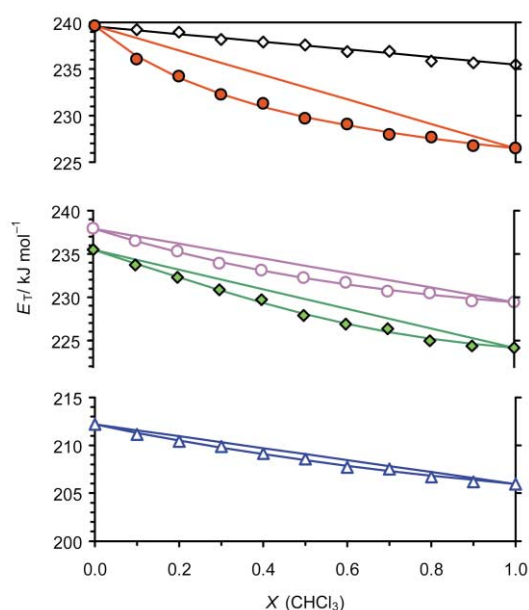
Fig. 1 Transition energies of the dyes **6** (◆), **7** (○), **8** (●), **9** (◇), and **10** (△) in binary mixtures of ethyl acetate–chloroform. Lines computed using eqn. (26) from the parameters in Table 4.
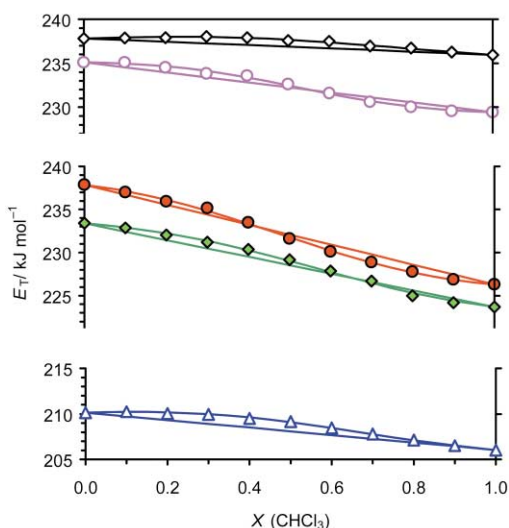
Fig. 2 Transition energies of the dyes **6–10** in binary mixtures of tri-*n*-butyl phosphate–chloroform. Symbols and lines as in Fig. 1.
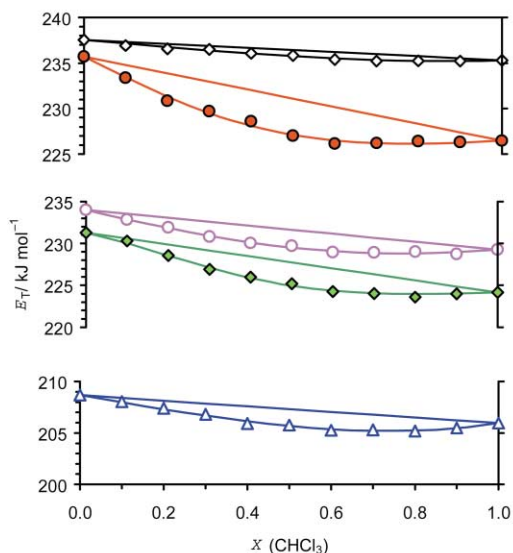

Fig. 3 Transition energies of the dyes **6–10** in binary mixtures of acetone–chloroform. Symbols and lines as in Fig. 1.

Fig. 4 Transition energies of the dyes **6–9** in binary mixtures of chloroform–methanol. Symbols and lines as in Fig. 1.

Fig. 5 Transition energies of the dyes **6–9** in binary mixtures of acetone–methanol. Symbols and lines as in Fig. 1.

dibromo quinone methide **10** has been omitted in mixtures with primary alcohols due to the band shape problems mentioned earlier. In most mixtures the isosolvation point was found to be higher than 0.5, when X_{iso} refers to the less polar solvent. Compound **9** in ethyl acetate–chloroform behaves ideally within experimental error but has $X_{iso} < 0.5$ in acetone–methanol. All dyes tested show an $E_{T, obs}$ minimum (polarity maximum) in chloroform–methanol, with E_{T12} being lower than E_{T1} and E_{T2}. The system tri-*n*-butyl phosphate–chloroform which reportedly has a polarity maximum,[21] behaved quite unexpectedly: the dyes **9** and **10** experience a lower than ideal polarity ($X_{iso} < 0.5$), whereas compounds **6–8** display a dual behaviour, as indicated by the s-shape of the curve.

X-Ray analysis

The bond lengths clearly show a quinoid system in compound **9**: double bonds O(1)=C(1) 124.3(3) pm, C(4)=C(7) 137.4(3) pm, C(2)=C(3) 134.5(3) pm, and single bonds C(3′)–C(7) 143.3(3) pm, C(1)–C(2) 147.9 pm, and C(3)–C(4) 143.4(3) pm. The angle between the quinone methide and guaiazulene planes is 41.6(1)°. The carbon atom of the isopropyl group attached to C(7′) in **9** is 1 : 1 disordered into two positions. This disorder also influences the ring carbon atoms in the vicinity of the
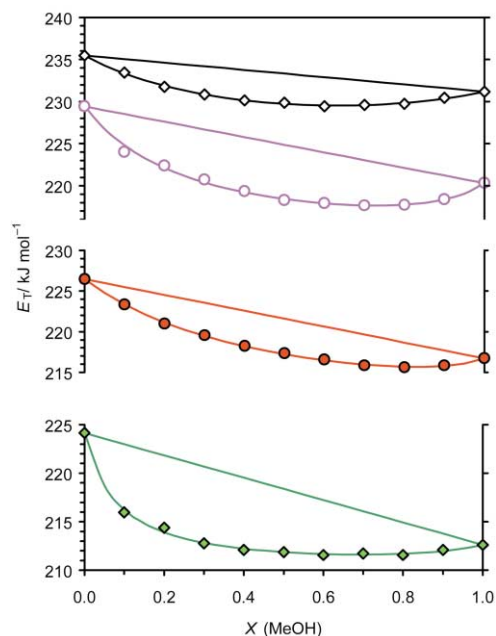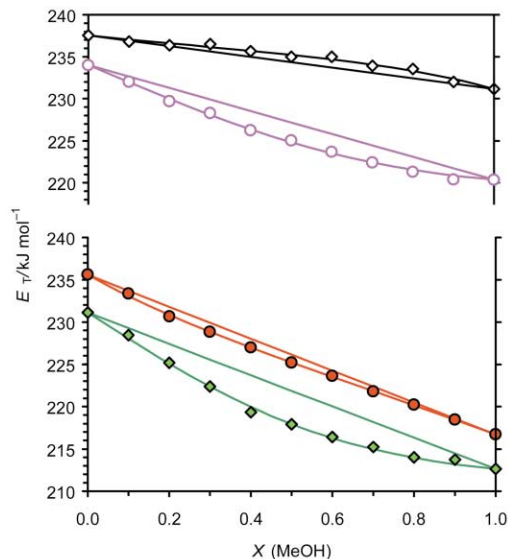
isopropyl group which show anomalously enlarged anisotropic displacement ellipsoids (Fig. 8).

In contrast, the phenolic cation **1** is planar (Fig. 9), and the single bond lengths are O(1)–C(1) 136.1(4) pm, C(4)–C(7) 144.2(5) pm, and double bond C(3′)=C(7) 136.4(5) pm.

IR analysis

The concept of linear solvation energy relationships has also been applied to infrared spectroscopy.[36] A solvent effect on the carbonyl stretching vibration of the quinone methides was expected. In a preliminary study of the C=O vibration wavenumber of compound **8** in nine solvents a satisfactory correlation was found (eqn. 27), indicating primarily sensitivity to the HBD capability of the solvent.
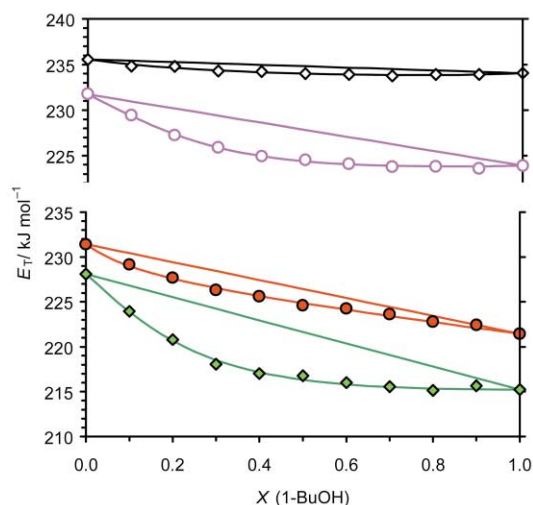
$$\tilde{v}_{max}/cm^{-1} = 1651.7(\pm2.3) - 19.3(\pm5.1)\pi^* - 123.9(\pm16.4)a \quad (27)$$

$r^2 = 0.964$, $\sigma/cm^{-1} = 3.06$ (rel. $\sigma = 0.19\%$), $N = 9$. The results are summarized in Table 5.

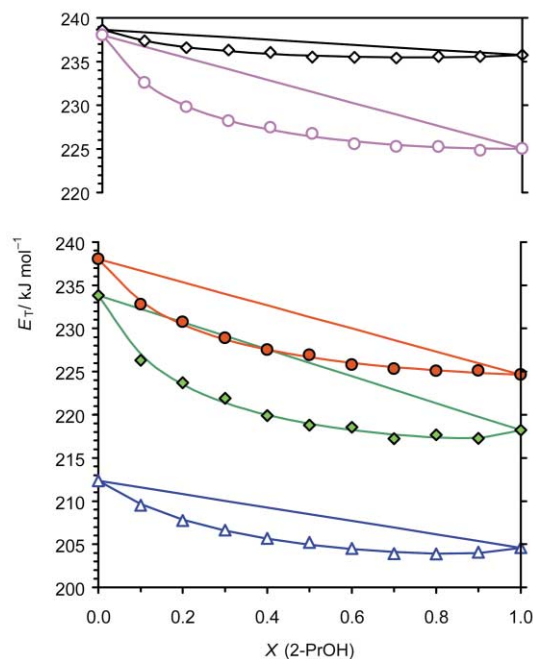| Solvent	$\tilde{\nu}/\text{cm}^{-1}$
Acetonitrile	1618.9
Dichloromethane	1618.9
Chloroform	1611.2
Tetrahydrofuran	1640.1
1,2-Dimethoxyethane	1638.2
Diethyl ether	1645.9
Carbon disulfide	1642.0
Triethylamine	1649.8
n-Hexane	1653.6

Fig. 6 Transition energies of the dyes **6**–**9** in binary mixtures of acetonitrile–butan-1-ol. Symbols and lines as in Fig. 1.


Fig. 7 Transition energies of the dyes **6**–**10** in binary mixtures of benzene–propan-2-ol. Symbols and lines as in Fig. 1.

Conclusion

We have studied the solvatochromic and halochromic properties of the new quinoid dyes **6**–**10** in various solvents. All dyes exhibit positive solvatochromism, the extent of which can be described by a linear combination of specific and non-specific solute–solvent interactions. The halochromism in organic solvents is dependent on the nature of the cation as well as the
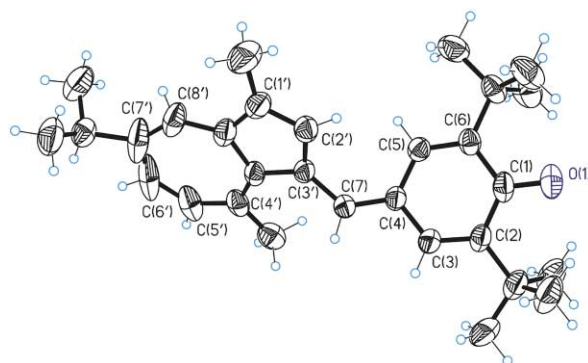
Fig. 8 ORTEP view of **9** with 40% displacement ellipsoids.
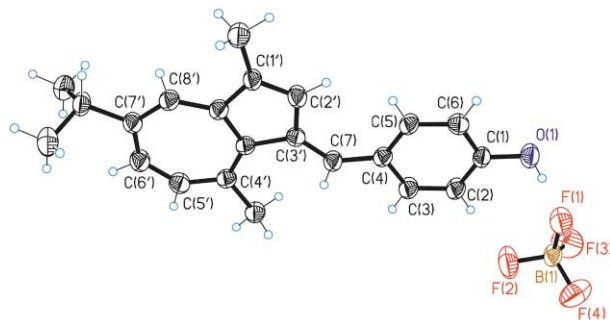
Fig. 9 ORTEP view of **1** with 40% displacement ellipsoids.

anion. The preferential solvation in mixtures of HBD and HBA solvents can be described by solvent–exchange models. Since these dyes are readily prepared, it can be expected that a number of analogues will be obtained in the future with potentially controlled properties and tailor-made sensitivities toward solvent and electrolyte interactions. Especially the dibromo aldehyde should represent a versatile precursor for the introduction of different substituents by metal-catalyzed cross couplings. It may also be of interest to use azulene instead of guaiazulene in the condensation reaction.

Experimental

The solvents and anhydrous salts were purchased in the highest purity available (Merck, Fluka, Aldrich). UV-VIS spectra were recorded using a Shimadzu UV-160A spectrophotometer equipped with a peak detection algorithm, which was calibrated using a solution of holmium perchlorate and thermostated at 25 °C. All measurements were taken at least in triplicate and averaged. The repeatability σ, estimated from 120 determinations of 40 samples, was 1.0 nm (corresponding to 0.4 kJ mol^{-1}); rel. σ 0.2%. Infrared spectra were obtained on a Nicolet 510 FT-IR instrument, and NMR spectra were recorded on Bruker AC 300 and Varian Gemini 200 spectrometers using tetramethylsilane as reference; shifts are given in ppm. *J* values are given in Hz. High resolution mass spectra (FAB: Cs gun, 3-nitrobenzyl alcohol matrix) were measured with a Varian MAT 95 spectrometer.

1-[(4-Hydroxyphenyl)methylene]guaiazulenium tetrafluoroborates (general procedure)

A solution of guaiazulene (1.78 g, 9.0 mmol) in anhydrous 1,2-dimethoxyethane (DME; 30 mL) is added dropwise to a solution of the respective 4-hydroxybenzaldehyde (10.0 mmol) and HBF$_4$ (3 mL, 54% solution in diethyl ether) in anhydrous DME (30 mL; 100 mL for the 3,5-dibromobenzaldehyde). The mixture is stirred for 1 hour at 0 °C. The resulting precipitate is filtered off, washed thoroughly with diethyl ether, and dried to give the respective 3-[(4-hydroxyphenyl)methylene]guaiazulenium tetrafluoroborates.

3-[(4-Hydroxyphenyl)methylene]guaiazulenium tetrafluoroborate (1). Red-brown plates (DME); yield: 80%; mp 202–208 °C; δ_H (300 MHz; acetone-d_6) 1.50 (d, 6H, J 7), 2.64 (s, 3H), 3.51 (s, 3H), 3.59 (sept, 1H, J 7), 7.13 (d, 2H, J 9), 8.00 (d, 2H, J 9), 8.31 (s, 1H), 8.58 (dd, 1H, J 11, J 2), 8.67 (d, 1H, J 11), 8.82 (d, 1H, J 2), 8.99 (s, 1H), 9.94 (s, 1H); $\tilde{v}_{max}$(KBr)/cm^{-1} 3398m, 2972w, 1605m, 1588m, 1565s, 1082m, 1048m; m/z 303.2 (M$^+$).

3-[(3,5-Dimethyl-4-hydroxyphenyl)methylene]guaiazulenium tetrafluoroborate (2). Dark purple microcrystalline powder (DME); yield: 89%; mp 199–205 °C; δ_H (300 MHz; acetone-d_6) 1.49 (d, 6H, J 7), 2.35 (s, 6H), 2.63 (s, 3H), 3.50 (s, 3H), 3.58 (sept, 1H, J 7), 7.79 (s, 2H), 8.38 (s, 1H), 8.54 (dd, 1H, J 2, J 11), 8.63 (d, 1H, J 11), 8.79 (d, 1H, J 2), 8.92 (s, 1H); $\tilde{v}_{max}$(KBr)/cm^{-1} 3423m, 2964w, 1602m, 1557s, 1293m, 1055m; m/z 331.2 (M$^+$).

3-[(3,5-Dimethoxy-4-hydroxyphenyl)methylene]guaiazulenium tetrafluoroborate (3). Dark purple microcrystalline powder (DME); yield: 77%; mp 194–199 °C; δ_H (300 MHz; acetone-d_6) 1.50 (d, 6H, J 7), 2.64 (s, 3H), 3.49 (s, 3H), 3.58 (sept, 1H, J 7), 7.41 (s, 2H), 8.38 (s, 1H), 8.56 (dd, 1H, J 11, J 2), 8.64 (d, 1H, J 11), 8.80 (d, 1H, J 2), 9.00 (s, 1H); $\tilde{v}_{max}$(KBr)/cm^{-1} 3388m, 2970w, 1605s, 1567s, 1511s, 1057s; m/z 363.2 (M$^+$).

3-[(3,5-Di-t-butyl-4-hydroxyphenyl)methylene]guaiazulenium tetrafluoroborate (4). Red-brown microcrystalline powder (DME); yield: 79%; mp 190–197 °C; δ_H (300 MHz; acetone-d_6) 1.49 (d, 6H, J 7), 1.51 (s, 18H), 2.65 (s, 3H), 3.49 (s, 3H), 3.57 (sept, 1H, J 7), 7.88 (s, 2H), 8.19 (s, 1H), 8.54 (d, 1H, J 11), 8.61 (d, 1H, J 11), 8.79 (d, 1H, J 2), 9.08 (s, 1H); $\tilde{v}_{max}$(KBr)/cm^{-1} 3620m, 2960m, 1576m, 1563s, 1057s; m/z 415.3 (M$^+$).

3-[(3,5-Dibromo-4-hydroxyphenyl)methylene]guaiazulenium tetrafluoroborate (5). Orange microcrystalline powder (DME); yield: 85%; mp 186–189 °C; δ_H (300 MHz; acetone-d_6) 1.51 (d, 6H, J 7), 2.64 (s, 3H), 3.54 (s, 3H), 3.64 (sept, 1H, J 7), 8.18 (s, 2H), 8.27 (s, 1H), 8.68 (dd, 1H, J 11, J 2), 8.79 (d, 1H, J 11), 8.86 (d, J 2, 1H), 8.90 (s, 1H); $\tilde{v}_{max}$(KBr)/cm^{-1} 3340m, 2977w, 1605m, 1594m, 1571s, 1476m, 1059s, 1001s; m/z 459.0 (M$^+$).

4-(Guaiazulen-3-ylmethylene)cyclohexa-2,5-dien-1-ones (general procedure)

A saturated solution of the respective salt **1**–**5** in CH$_2$Cl$_2$ is shaken with saturated aqueous NaHCO$_3$ solution, washed with deionized water, dried with anhydrous Na$_2$SO$_4$, and the solvent is evaporated at room temperature under reduced pressure. The residue is dried *in vacuo*. A quantitative yield of the quinone methide is obtained.

4-(Guaiazulen-3-ylmethylene)cyclohexa-2,5-dien-1-one (6). Dark blue microcrystalline powder (CH$_2$Cl$_2$); mp 129–130 °C (decomp.); δ_H (300 MHz; chloroform-d_1) 1.38 (d, 6H, J 7), 2.61, 3.08, 3.12 (sept, 1H, J 7), 6.59 (d, 2H, J 9), 7.27 (d, 2H, J 9), 7.56 (dd, 1H, J 11, J 2), 7.63 (d, 1H, J 11), 7.84 (s, 1H), 8.18 (d, 1H, J 2), 8.21 (s, 1H); $\tilde{v}_{max}$(KBr)/cm^{-1} 2960m, 2919m, 1603m, 1499s, 1158s; HR-MS (FAB): m/z 303.1749 (M + H$^+$); C$_{22}$H$_{23}$O requires 303.1743.

2,6-Dimethyl-4-(guaiazulen-3-ylmethylene)cyclohexa-2,5-dien-1-one (7). Dark purple microcrystalline powder (CH$_2$Cl$_2$); mp 150–152 °C (decomp.); δ_H (300 MHz; acetone-d_6) 1.35 (d, 6H, J 7), 2.00 (s, 6H), 2.62 (s, 3H), 3.06 (s, 3H), 3.15 (sept, 1H, J 7), 7.24 (d, 1H, J 11), 7.26 (s, 1H), 7.52 (s, 1H), 7.58 (dd, 1H, J 2, J 11), 7.86 (s, 1H), 8.13 (s, 1H), 8.25 (d, 1H, J 2); $\tilde{v}_{max}$(KBr)/cm^{-1} 2958m, 2919w, 1629m, 1598m, 1526s, 1507s, 1391m, 1364m, 1320m, 1246m, 1038m; HR-MS (FAB): m/z 331.2061 (M + H$^+$); C$_{24}$H$_{27}$O requires 331.2056.

2,6-Dimethoxy-4-(guaiazulen-3-ylmethylene)cyclohexa-2,5-dienone (8). Dark purple microcrystalline powder (CH$_2$Cl$_2$); mp 88–90 °C (decomp.); δ_H (200 MHz; acetone-d_6) 1.35 (d, 6H, J 7), 2.62 (s, 3H), 3.04 (s, 3H), 3.12 (sept, 1H, J 7), 3.76 (s, 6H), 6.94 (s, 2H), 7.15 (d, 1H, J 11), 7.51 (dd, 1H, J 2, J 11), 7.89 (s, 1H), 8.06 (s, 1H), 8.21 (d, 1H, J 2); δ_H (300 MHz; chloroform-d_1) 1.35 (d, 6H, J 7), 2.62 (s, 3H), 3.04 (s, 3H), 3.06 (sept, 1H, J 7), 3.80 (s, 3H), 3.84 (s, 3H), 6.52 (s, 1H), 7.04 (s, 1H), 7.10 (d, 1H, J 11), 7.42 (dd, 1H, J 2, J 11), 7.76 (s, 1H), 7.92 (s, 1H), 8.12 (d, 1H, J 2); $\tilde{v}_{max}$(KBr)/cm^{-1} 2956w, 2927w, 1629s, 1511m, 1324s, 1262m, 1113s; $\tilde{v}_{max}$(C=O, solvent)/cm^{-1} 1611.2 (CHCl$_3$), 1618.9 (CH$_3$CN), 1618.9 (CH$_2$Cl$_2$), 1640.1 (THF), 1638.2 (DME), 1645.9 (Et$_2$O), 1642.0 (CS$_2$), 1649.8 (Et$_3$N), 1653.6 (*n*-hexane); HR-MS (FAB): m/z 363.1954 (M + H$^+$); C$_{24}$H$_{27}$O$_3$ requires 363.1955.

2,6-Di-t-butyl-4-(guaiazulen-3-ylmethylene)cyclohexa-2,5-dien-1-one (9). Dark red platelets (CH$_2$Cl$_2$); mp 176–180 °C (decomp.); δ_H (300 MHz; acetone-d_6) 1.32 (s, 9H), 1.34 (s, 9H), 1.36 (d, J 7, 6H), 2.63 (s, 3H), 3.06 (s, 3H), 3.15 (sept, 1H, J 7), 7.23 (d, 1H, J 11), 7.30 (d, 1H, J 2), 7.57 (dd, 1H, J 11, J 2), 7.73 (d, 1H, J 2), 7.81 (s, 1H), 8.22 (s, 1H), 8.25 (d, 1H, J 2); $\tilde{v}_{max}$(KBr)/cm^{-1} 2958m, 2912w, 1619w, 1596s, 1536s, 1515s, 1403s, 1356m, 1088m, 1030m; HR-MS (FAB): m/z 415.2982 (M + H$^+$); C$_{30}$H$_{39}$O requires 415.2995.

2,6-Dibromo-4-(guaiazulen-3-ylmethylene)cyclohexa-2,5-dien-1-one (10). Dark purple microcrystalline powder (CH$_2$Cl$_2$); mp 177–180 °C (decomp.); δ_H (300 MHz; acetone-d_6) 1.40 (d, 6H, J 7), 2.64 (s, 3H), 3.22 (s, 3H), 3.26 (sept, 1H, J 7), 7.64 (d, 1H, J 11), 7.84 (dd, 1H, J 11, J 2), 8.04 (br s, 1H), 8.08 (s, 1H), 8.41 (br s, 1H), 8.42 (d, 1H, J 2), 8.58 (s, 1H); $\tilde{v}_{max}$(KBr)/cm^{-1} 2923w, 2858w, 1602m, 1534s, 1517m, 1391m, 1362m, 1289m, 1248m, 1196m, 1040m; HR-MS (FAB): m/z 458.9938 (M+H$^+$); C$_{22}$H$_{21}$Br$_2$O requires 458.9954.

Crystal data determinations of compounds 1 and 9 ‡

Diffraction intensity data were collected using a Nonius Kappa CCD with graphite-monochromatized MoK$_\alpha$ radiation (λ = 71.073 pm) *via* ϕ- and ω-scans. The structures were solved with direct methods (SHELXS-86) and refined against F^2 (SHELXL-97). Hydrogen atoms at carbon atoms were added geometrically and refined using a riding model, the hydrogen atom of the hydroxy group of **1** was refined with isotropic displacement parameters. All non-hydrogen atoms were refined with anisotropic displacement parameters.

Crystal data of 1. Red plate (0.25 × 0.1 × 0.04 mm) from dichloromethane, C$_{22}$H$_{23}$BF$_4$O, M = 390.2, monoclinic, a = 985.32(7), b = 699.44(5), c = 1450.4(1) pm; $\alpha = \gamma$ = 90°, β = 105.737(3)°, V = 0.96211(12) nm^3, T = 233 K, space group $P2(1)/m$, Z = 2, μ = 0.107 mm^{-1}, 4286 reflections measured, 1215 independent (R_{int} = 0.0427), 945 observed, R_1 = 0.0423 and wR_2 = 0.0992 ($I>2\sigma(I)$), R_1 = 0.0595 and wR_2 = 0.1067 (all data).

Crystal data of 9. Red prism (0.3 × 0.3 × 0.3 mm) from *iso*-pentane, C$_{30}$H$_{38}$O, M = 414.6, monoclinic, a = 1432.40(9), b = 1255.01(7), c = 1462.3(1) pm; $\alpha = \gamma$ = 90°, β = 100.000(3)°, V = 2.5888(3) nm^3, T = 228 K, space group $P2(1)/c$, Z = 4, μ = 0.062 mm^{-1}, 10312 reflections measured, 2786 independent (R_{int} = 0.0357), 2198 observed, R_1 = 0.0505 and wR_2 = 0.1306 ($I>2\sigma(I)$), R_1 = 0.0665 and wR_2 = 0.1409 (all data).

References

1 C. Reichardt, *Solvents and Solvent Effects in Organic Chemistry*, 2nd edn., VCH, Weinheim, 1990.

2 C. Reichardt, *Chem. Rev.*, 1994, **94**, 2319–2358.

3 J.-L. M. Abboud, R. W. Taft and M. J. Kamlet, *J. Chem. Soc., Perkin Trans. 2*, 1985, 815–819.

4 S. Ito, S. Kikuchi, H. Kobayashi, N. Morita and T. Asao, *J. Org. Chem.*, 1997, **62**, 2423–2431.

5 M. J. Kamlet, J.-L. M. Abboud, M. H. Abraham and R. W. Taft, *J. Org. Chem.*, 1983, **48**, 2877–2887.

6 M. J. Kamlet, T. N. Hall, J. Boykin and R. W. Taft, *J. Org. Chem.*, 1979, **44**, 2599–2604; M. J. Kamlet, J.-L. M. Abboud and R. W. Taft, *J. Am. Chem. Soc.*, 1977, **99**, 6027–6038.

7 R. W. Taft and M. J. Kamlet, *J. Am. Chem. Soc.*, 1976, **98**, 2886–2894.

8 M. J. Kamlet and R. W. Taft, *J. Am. Chem. Soc.*, 1976, **98**, 377–383.

9 R. W. Taft, J.-L. M. Abboud and M. J. Kamlet, *J. Am. Chem. Soc.*, 1981, **103**, 1080–1086.

10 J. Catalán, *J. Org. Chem.*, 1995, **60**, 8315–8317.

11 F. Effenberger, F. Würthner and F. Steybe, *J. Org. Chem.*, 1995, **60**, 2082–2091.

12 C. Reichardt, S. Asharin-Fard and G. Schäfer, *Chem. Ber.*, 1993, **126**, 143–147.

13 M. C. Rezende, *Tetrahedron*, 1988, **44**, 3513–3522.

14 V. Gageiro, M. Aillon and M. C. Rezende, *J. Chem. Soc., Faraday Trans.*, 1992, **88**, 201–204.

15 G. Hollmann and F. Vögtle, *Chem. Ber.*, 1984, **117**, 1355–1363; C. Machado, M. da G. Nascimento and M. C. Rezende, *J. Chem. Soc., Perkin Trans. 2*, 1994, 2539–2544.

16 C. B. Ramirez, N. Carrasco and M. C. Rezende, *J. Chem. Soc., Faraday Trans.*, 1995, **91**, 3839–3842.

17 H. Langhals, *Tetrahedron*, 1987, **43**, 1771–1774.

18 Y. Pocker and J. C. Ciula, *J. Am. Chem. Soc.*, 1989, **111**, 4728–4735.

19 H. Langhals, *Angew. Chem.*, 1982, **21**, 739–749; H. Langhals, *Chem. Ber.*, 1981, **114**, 2907–2913.

20 M. C. Rezende, D. Zanette and C. Zucco, *Tetrahedron Lett.*, 1984, **25**, 3423–3424.

21 M. Rosés, C. Ráfols, J. Ortega and E. Bosch, *J. Chem. Soc., Perkin Trans. 2*, 1995, 1607–1615.

22 J. Ortega, C. Ráfols, E. Bosch and M. Rosés, *J. Chem. Soc., Perkin Trans. 2*, 1996, 1497–1503; K. Herodes, I. Leito, I. Koppel and M. Rosés, *J. Phys. Org. Chem.*, 1999, **12**, 109–115.

23 E. B. Tada, L. P. Novaki and O. A. El Seoud, *J. Phys. Org. Chem.*, 2000, **13**, 679–687.

24 C. Ráfols, M. Rosés and E. Bosch, *J. Chem. Soc., Perkin Trans. 2*, 1997, 243–248; E. Bosch, F. Rived and M. Rosés, *J. Chem. Soc., Perkin Trans. 2*, 1996, 2177–2184.

25 P. M. Mancini, C. Adam, A. del C. Perez and L. R. Vottero, *J. Phys. Org. Chem.*, 2000, **13**, 221–231.

26 S. Balakrishnan and A. J. Easteal, *Aust. J. Chem.*, 1981, **34**, 933–941; S. Balakrishnan and A. J. Easteal, *Aust. J. Chem.*, 1981, **34**, 943–947.

27 A. Taha and A. M. Kiwan, *New J. Chem.*, 2001, **25**, 502–508.

28 A. K. Laha, P. K. Das and S. Bagchi, *J. Phys. Chem. A*, 2002, **106**, 3230–3234.

29 A. Taha, A. A. T. Ramadan, M. A. El-Behairy, A. I. Ismail and M. M. Mahmoud, *New J. Chem.*, 2001, **25**, 1306–1312.

30 V. Gageiro Machado, C. Machado, M. de G. Nascimento and M. C. Rezende, *J. Phys. Org. Chem.*, 1997, **10**, 731–736.

31 D. J. Phillips and J. F. Brennecke, *Ind. Eng. Chem. Res.*, 1993, **32**, 943–951.

32 P. Chatterjee and S. Bagchi, *J. Phys. Chem.*, 1991, **95**, 3311–3314.

33 R. D. Skwierczynski and K. A. Connors, *J. Chem. Soc., Perkin Trans. 2*, 1994, 467–472.

34 W. E. Acree, J. R. Powell and S. A. Tucker, *J. Chem. Soc., Perkin Trans. 2*, 1995, 529–531.

35 L. S. Frankel, C. H. Langford and T. R. Stengle, *J. Phys. Chem.*, 1970, **74**, 1376–1381.

36 M. J. Kamlet and R. W. Taft, *J. Chem. Soc., Perkin Trans. 2*, 1979, 337–341.

37 Y. Marcus, *Chem. Soc. Rev.*, 1993, **22**, 409–416.